angle which the normal to the nonlinear wavefront (which we shall refer to simply as the front) at time t makes with a fixed direction, say the x-axis.

The position of the wavefront at time t is given parametrically by $(x(\xi, t), y(\xi, t))$, where ξ is chosen such that when ξ is fixed and t varies we move along a ray. Then (ξ, t) represents a ray coordinate system. We note that for the waves under consideration, the ξ = constant curves and the t = constant curves form an orthogonal system. Therefore, a point on the ray moving with the wavefront satisfies

$$x_t = m\cos\theta, \quad y_t = m\sin\theta. \tag{1}$$

m is the metric along the rays, i.e. $m\,dt$ represents an element of distance along a ray in the (x, y)-plane. Let g be a function such that $g\,d\xi$ is an element of distance along the wavefront. Morton *et al.* showed that the equations of the weakly nonlinear ray theory (WNLRT) for m and θ can be written as conservation laws[5]

$$(g\sin\theta)_t + (m\cos\theta)_\xi = 0, \tag{2}$$

and

$$(g\cos\theta)_t - (m\sin\theta)_\xi = 0, \tag{3}$$

where g satisfies

$$g = (m-1)^{-2}\, e^{-2(m-1)}. \tag{4}$$

Equations (1) to (4) form the complete set of equations of our WNLRT. Though the expression for g is actually given as $g = f(\xi)(m-1)^{-2}\, e^{-2(m-1)}$, where $f(\xi)$ depends on the initial position of the wavefront and amplitude distribution m on it, we can choose ξ suitably[5] (as a function of the arclength along the wavefront) so that $f(\xi) = 1$. Then $g(\xi, 0)$ is determined from eq. (4) and we can set up an initial value problem for the eqs (1) to (3):

$$x(\xi, 0) = x_0(\xi), \quad y(\xi, 0) = y_0(\xi), \tag{5}$$

$$m(\xi, 0) = m_0(\xi) \text{ and } \theta(\xi, 0) = \theta_0(\xi). \tag{6}$$

Equations (2) and (3) with initial conditions (6) can be solved first and then the position of the wavefront at any time can be found by integrating (1) with respect to t (i.e. along the rays) with initial condition (5).

The system, eqs (2) and (3), is hyperbolic when $m > 1$, i.e. when the gas pressure in the wave is greater than that in the unperturbed medium. We restrict our discussion only to the situation when $m > 1$. The characteristic curves are

$$\begin{aligned} d\xi/dt &= -\sqrt{\{(m-1)/(2g^2)\}} = \lambda_1, \text{ say;} \\ d\xi/dt &= \sqrt{\{(m-1)/(2g^2)\}} = \lambda_2, \text{ say.} \end{aligned} \tag{7}$$

An interesting exact solution of eqs (1) to (6) is available[5] using two receding simple waves in $\xi < 0$ and $\xi > 0$. The

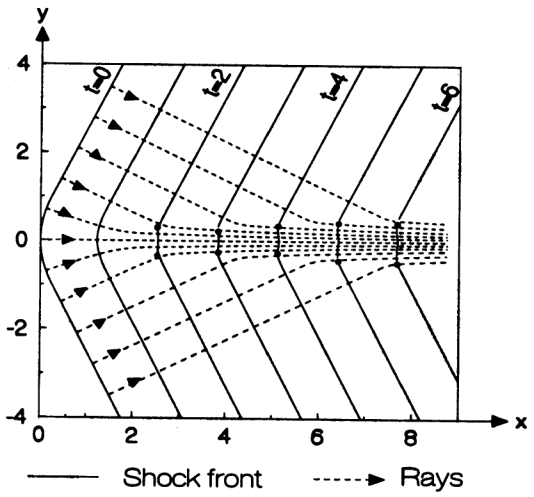

Figure 2. Successive positions of a shock front starting from an initial shape of the type shown in Figure 1. Rays are shown by broken lines and kinks by dots.

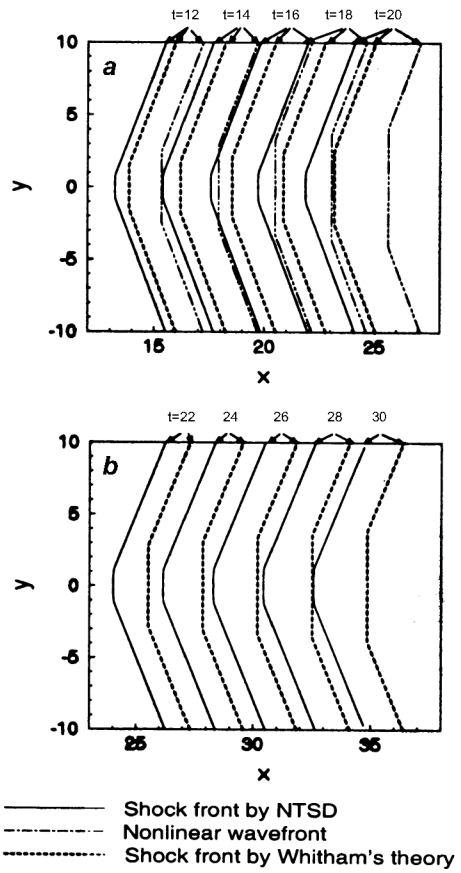

Figure 3. Comparison of the successive positions of the shock fronts (by NTSD and Whitham's theory) and a nonlinear wavefront starting with same initial front ($y^2 = 8x$ for $0 < x < 1$ and $y - 1 = \pm(4x - 0.5)$ for $x > 1$) and same initial amplitude distribution.

solution shows that the caustic is completely resolved due to nonlinearity and the wavefront emerges unfolded. Further, extensive numerical solutions[6] of these equations again lead to the same result: converging rays starting from concave parts of an initial wavefront are not allowed to converge due to nonlinearity and the nonlinear wavefront, which emerges unfolded, develops kinks. Kinks are images in the (x, y)-plane of shocks in (ξ, t)-plane of the conservation laws (2) and (3). Figure 3 shows results of one numerical computation showing the shapes of a nonlinear wavefront[6] and a shock front by the new theory of shock dynamics (NTSD)[7] verifying the assertion that geometrical features of these two types of fronts are qualitatively similar. For a shock front by NTSD, we need an additional initial data which is the distribution of normal derivative of a quantity (say density) behind the shock.

Elementary wave solutions and their interpretation as elementary shapes

Elementary wave solutions of eqs (2) and (3) are solutions of the form $m(\xi, t) = m(\xi/t)$, $\theta(\xi, t) = \theta(\xi/t)$. These are centred rarefaction wave solutions with centre at the origin and shock waves passing through the origin.

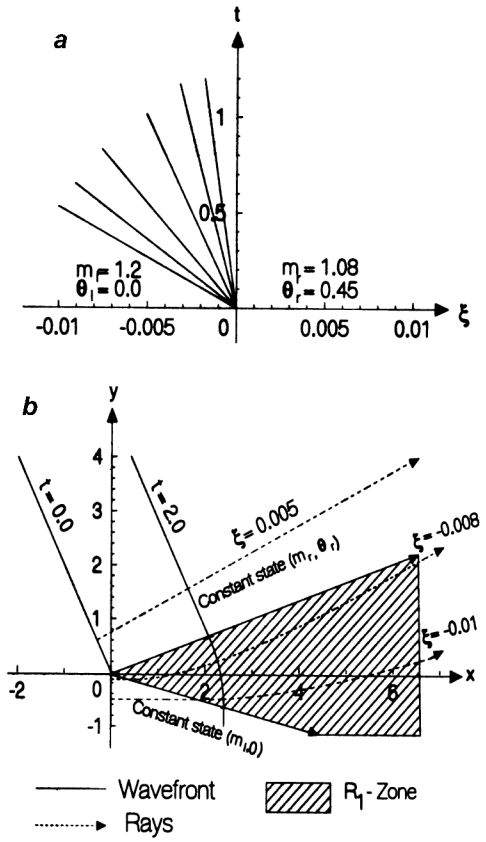

Figure 4. *a*, Example of the 1-R wave, i.e. centred simple wave of the first family in the (ξ, t)-plane. The fan of characteristic curves is shown; *b*, Geometrical features of the front associated with the solution in *a*.

We denote centred rarefaction waves of first and second characteristic family by 1-R and 2-R, respectively. In a 1-R wave, the corresponding Riemann invariant is constant, i.e. $\theta + \sqrt{(8(m-1))}$ = constant. Suppose the constant state on the left of the 1-R wave in the (ξ, t)-plane is (m_l, θ_l), then by rotation of the coordinate axes we can always choose $\theta_l = 0$, i.e. for the 1-R wave we have (see relation (6.57), ref. 5)

$$\theta + \sqrt{(8(m-1))} = \sqrt{(8(m_l - 1))}. \tag{8}$$

If the state on any straight characteristic in the 1-R wave in the (ξ, t)-plane be (m, θ), then $\lambda_1(m_l) < \lambda(m)$ which implies $m_l > m$. Then the relation (8) gives $\theta > 0$. At the trailing end of the 1-R wave in ξ-space, the wave merges into a constant state (m_r, θ_r) and these inequalities remain valid i.e. $m_r < m_l$ and $\theta_r > 0$. Figure 4 *a* represents a typical 1-R wave solution in the (ξ, t)-plane and Figure 4 *b* represents its image in the (x, y)-plane. Similarly, Figure 5 *a* represents a typical 2-R wave solution in the (ξ, t)-plane and Figure 5 *b* its image in the (x, y)-plane, where we note that that $m_r > m_l$ and $\theta_r > 0$. We call a shape of a front in the (x, y)-plane obtained from an elementary wave

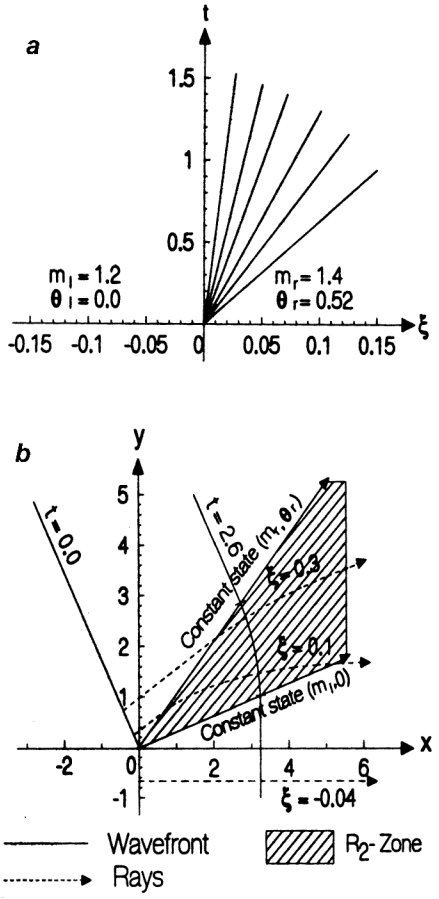

Figure 5. *a*, Example of the 2-R wave, i.e. centred simple wave of the second family in the (ξ, t)-plane. The fan of characteristic curves is shown; *b*, Geometrical features of the front associated with the solution in *a*.

solution in the (ξ, t)-plane as an *elementary shape*. We observe that the elementary shapes in Figure 4 *b* (we denote it by R_1) and Figure 5*b* (we denote it by R_2) are convex smooth wavefronts and look almost the same geometrically but R_1 in Figure 4 *b* propagates downwards on the wavefront whereas R_2 in Figure 5 *b* moves upwards. Note that the rays in Figure 4 *b* cross the R_1 region from below whereas in Figure 5 *b* they cross R_2 from above.

When $(m_l, 0)$ and (m_r, θ_r) satisfy appropriate jump conditions (see relation (6.67), reference 5), we get one of the two shocks 1-S and 2-S joining two constant states $(m_l, 0)$ and (m_r, θ_r) and passing through $\xi = 0$ at $t = 0$. The jumps in θ and m across a shock satisfy (since $\theta_l = 0$)

$$\cos\theta_r = (m_r g_r + m_l g_l)/(m_l g_r + m_r g_l). \tag{9}$$

Since the Lax shock inequality implies $\lambda_1(m_r) < \lambda_1(m_l)$ for 1-S and $\lambda_2(m_r) < \lambda_2(m_l)$, for 2-S, we get $m_r > m_l$ for 1-S and $m_r < m_l$ for 2-S. From the expression for g it follows that g decreases after crossing the shock ($g_r < g_l$ for 1-S and $g_r > g_l$ for 2-S). The jump relations from (2.2) and (2.3) give

$$s g_r \sin\theta_r = g_r(m_r^2 - m_l^2)/(m_l g_r + m_r g_l), \tag{10}$$

where s is the shock velocity in the (ξ, t)-plane which is negative for 1-S and positive for 2-S. This relation shows that for both shocks $\theta_r < 0$. The images of 1-S and 2-S in the (ξ, t)-plane to the (x, y)-plane are elementary shapes of a front, which are 1-kink (denoted by K_1) and 2-kink (denoted by K_2) as shown in Figure 6 *a* and Figure 6 *b*, respectively.

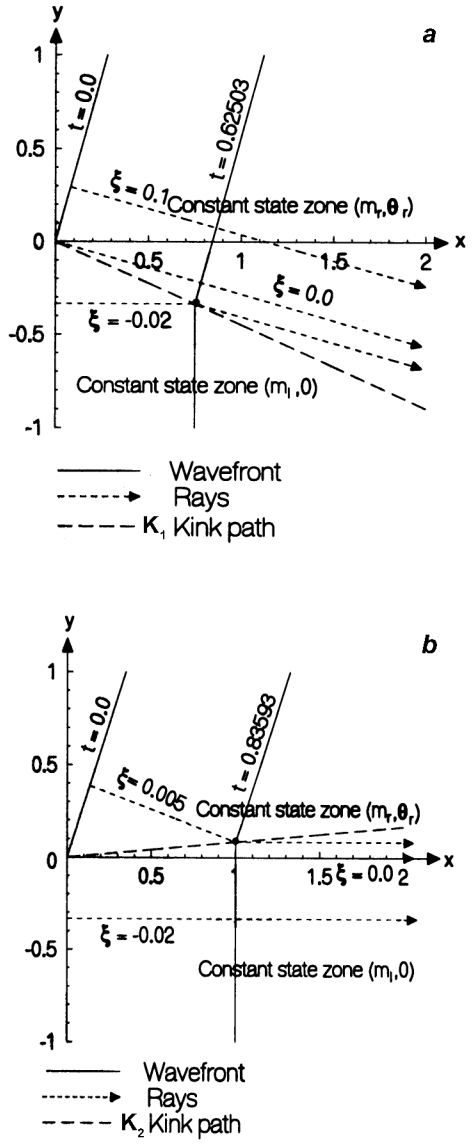

Figure 6 *a*, *b*. Rays are neither created nor lost across a kink but suddenly change their direction and since g decreases after it crosses the kink path, the rays emerge compressed.

Solution of the Reimann problem and interpretation

In this section we briefly review some recent work of Baskar, Potadar and Szeftel (1999). A Riemann problem for the system, eqs (2) and (3) consists of solving the system with following initial conditions

$$(m,\theta)\,|_{t=0} = \begin{cases} (m_l, \theta_l), & \text{we choose } \theta_l = 0, \xi < 0, \\ (m_l, \theta_r), & \xi > 0, \end{cases} \tag{11}$$

where m_l, m_r and θ_r are constant.

We define curves R_α and S_α ($\alpha = 1, 2$) as loci of the points (m_r, θ_r) which can be joined to the point $(m_l, 0)$ by α-R and α-S waves. Figure 7 shows these curves for a typical value of $m_l = 1.2$. We note that nonlinear ray theory is valid only for small values of $m - 1$, say for $0 < m - 1 < 0.25$.

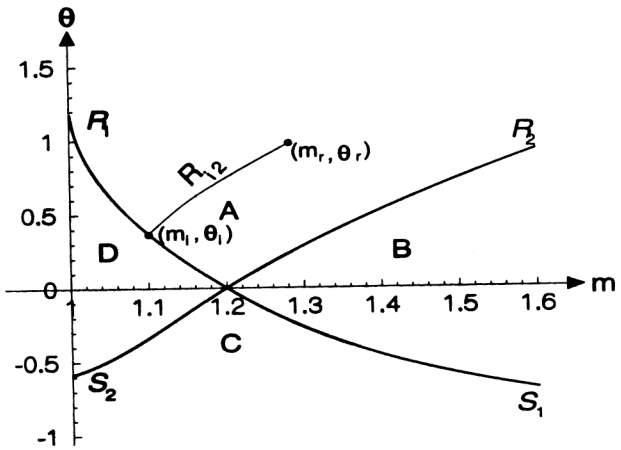

Figure 7. R_α and S_α ($\alpha = 1, 2$) curves in the (m, θ)-plane for $m = 1.2$.

If we do not go into the question of existence of the curves into consideration, the method of solution of the Riemann problem is simple. Suppose (m_r, θ_r) lies in the domain A bounded by curves R_1 and R_2 as shown in Figure 7. We draw a curve R_{i2} which represents the set of points joining (m_r, θ_r) by 2-R wave to an intermediate state (m_i, θ_i), which lies on the R_1 curve. Thus, in this case the solution consists of the state $(m_l, 0)$ on the left of a 1-R wave continuing up to an intermediate constant state (m_i, θ_i), which ends into a 2-R wave to the right of which we have the final state (m_r, θ_r) (see Figure 8 *a*). The shape of the wavefront at $t = 0$ and $t = t_1 > 0$ is shown in Figure 8 *b*. Since $(m_l, 0)$ is a state on the left, it can be joined to an intermediate state (m_i, θ_i) on its right only if (m_i, θ_i) lies on R_1 and not on R_2.

We describe this result symbolically as

$$(m_r, \theta_r) \in A \rightarrow \mathrm{R}_1\mathrm{R}_2, \tag{12}$$

which means that when (m_r, θ_r) is in A, the resultant wavefront has an elementary shape R_1 propagating below, and R_2 propagating above and these two are separated by a section of plane (or straight) front. Similarly we get the result

$$(m_r, \theta_r) \in B \rightarrow \mathrm{K}_1\mathrm{R}_2, \tag{13}$$

as shown in Figure 9. Other results are,

$$(m_r, \theta_r) \in C \rightarrow \mathrm{K}_l\mathrm{K}_2, \tag{14}$$

$$(m_r, \theta_r) \in D \rightarrow \mathrm{R}_l\mathrm{K}_2. \tag{15}$$

Asymptotic result of a nonlinear wavefront[6] when the initial wavefront is as in Figure 2 can be easily obtained. We note that when we observe the wavefront from a very large length scale, the central curved part of the initial wavefront tends to a point and the initial data reduces to

$$m(\xi, 0) = \begin{cases} (m_l, \theta_l) & \xi < 0, \\ (m_l, -\theta_l) & \xi > 0. \end{cases} \tag{16}$$

Choosing the direction of the x-axis perpendicular to the lower part the wavefront, solving the corresponding Riemann problem and rotating back the x-direction we get the following solution of eqs (2), (3) and (16)

$$m(\xi, t) = \begin{cases} (m_l, \theta_l) & \xi < -st, \\ (m_i, 0) & -st < \xi < st, \\ (m_l, -\theta_l) & st < \xi, \end{cases} \tag{17}$$

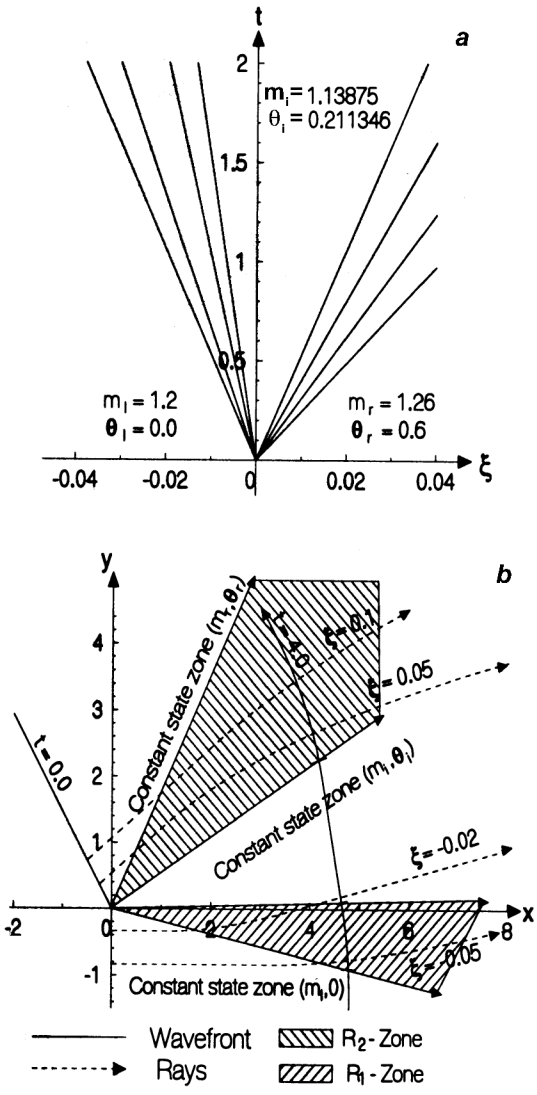

Figure 8. *a*, Solution of the Riemann problem when (m_r, θ_r) is in A; *b*, Shape of the wavefront at $t = 0$ and $t = t_1 > 0$ when (m_r, θ_r) is in A.

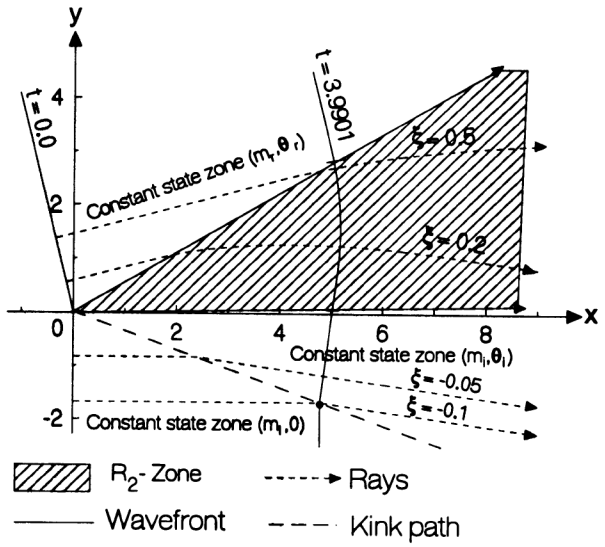

Figure 9. When (m_r, θ_r) is in B, the front consists of a K_1 propagating downward and R_2 propagating upward.

where m_i is given by the equation

$$m_i g_{mi} + m_l g_{ml} = (m_i g_{ml} + m_l g_{mi}) \cos\theta_l, \tag{18}$$

and

$$s = \sqrt{\{(m_i^2 - m_l^2)/(g_{ml}^2 - g_{mi}^2)\}}. \tag{19}$$

This solution when mapped into the (x, y)-plane gives the shape of the wavefront as shown in Figure 10.

Transition from one shape of the wavefront to another shape (e.g. from R_1R_2 to K_1R_2) as the point (m_r, θ_r) crosses curves R_1, R_2, S_1 or S_2 has also been discussed. The results of transitions lead to beautiful geometrical patterns.

Interaction of elementary shapes

Elementary shapes on a nonlinear wave propagate on the front. Two elementary shapes, separated by a plane portion of the front, may or may not interact. The process of interaction may take finite or infinite time depending on the strengths of the two elementary shapes. It is not possible to visualize the shape during the process of interaction without full numerical solution of the conservation laws, eqs (2) and (3). However, when the interaction period is finite we can easily obtain the final results, which will again consist of a pair of elementary shapes. All these geometrically beautiful results can be studied from the corresponding results on the interaction of simple waves and shock waves in the (ξ, t)-plane[12,13]. We can use Figure 7 for this purpose, where we note that the curves R_1, R_2, S_1 and S_2 are meaningful for more general simple waves (not just for centred waves) and shock waves (not necessarily passing through the origin in the (ξ, t)-plane). No distinction has been made between the waves, in which characteristics converge (corresponding to compression waves

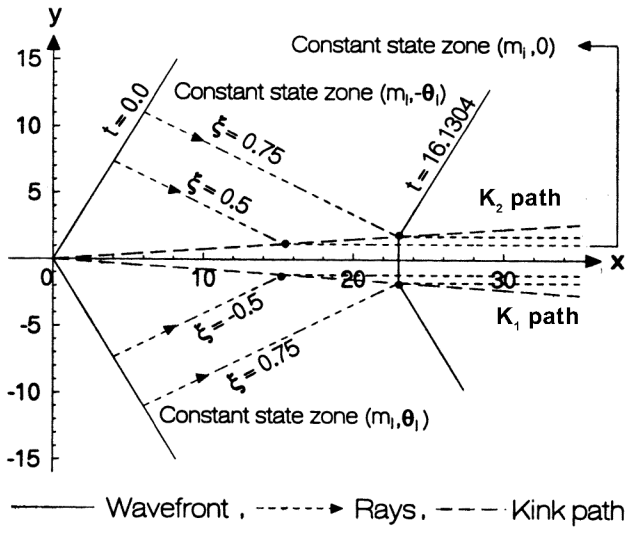

Figure 10. Limiting shape, as t tends to infinity, of the nonlinear wavefront originating from an initial front as in Figure 2.

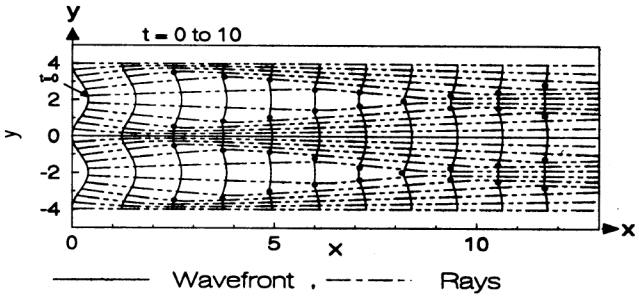

Figure 11. Successive positions of an initially sinusoidal shock front and rays plotted at $t = 0, 1, 2, \ldots, 10$. Kinks have been shown by dots.

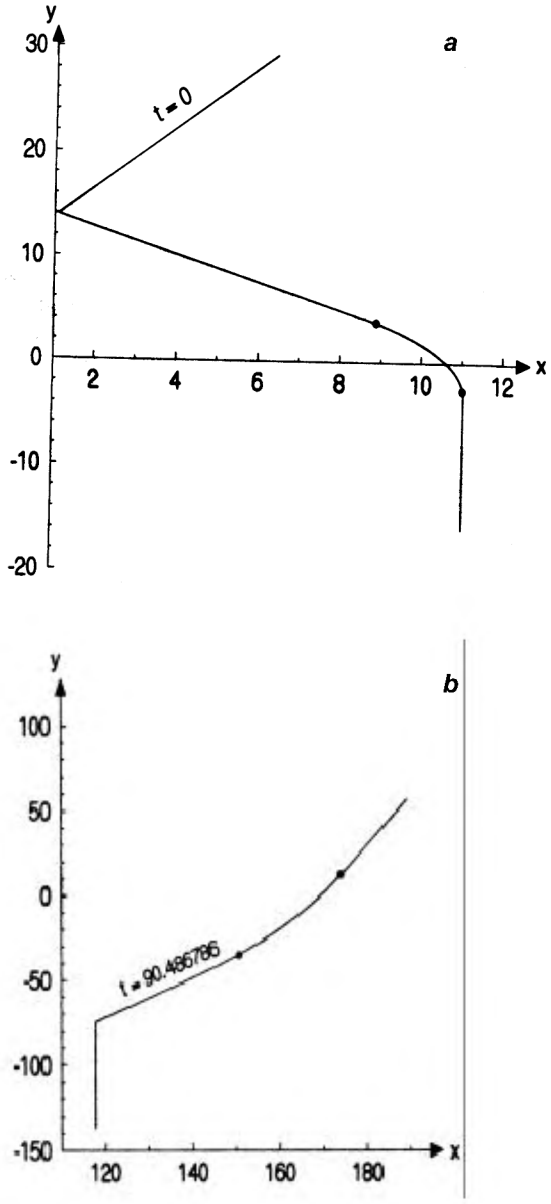

Figure 12. *a*, The front R_1K_1 before the interaction; *b*, The front K_1R_2 after the interaction.

in gas dynamics), and a corresponding shock. This is justified because we are considering only small changes in m. We use the symbols introduced in the previous section with a slight modification. K_2K_1 would mean a kink of second family on the lower part of the front (smaller values of ξ) separated by a plane part (m_j, θ_j) of the front from a kink of the first family on the upper part of the front. To reach a state (m_r, θ_r) from $(m_1, 0)$ through K_2K_1, we need to move along S_2 from $(m_1, 0)$ up to (m_j, θ_j) and then move along S_{j1} from (m_j, θ_j) up to the point $(m_r\, \theta_r)$. Clearly (m_r, θ_r) is in the region C, which implies

$$K_2K_1 \rightarrow K_1K_2, \tag{20}$$

with obvious physical interpretation. Such interactions of kinks are clearly seen in the case of propagation of an initially sinusoidal front[7], reproduced here in Figure 11.

All possible interactions of elementary shapes, namely K_1K_1, K_2K_2, R_1K_1, R_2K_2, K_1R_1, K_2R_2, R_2R_1, R_2K_1 and K_2R_1 in addition to K_2K_1 mentioned earlier, have been discussed. A geometrical representation of one of these cases, namely

$$R_1K_1 \rightarrow K_1R_2$$

when K_1 is strong compared to R_1 has been shown in Figure 12. Note that the scales for x and y used in Figure 12 *a* and *b* are very different.

1. Sturtevant, B. and Kulkarni, V. A., *J. Fluid Mech.*, 1976, **73**, 651–671.
2. Whitham, G. B., *Linear and Nonlinear Waves*, Wiley, 1974.
3. Ramanathan, T. M., Ph D thesis, Indian Institute of Science, Bangalore, 1985.
4. Ravindran, R. and Prasad, P., *Advances in Nonlinear Waves* (ed. Debnath, L.), Pitman, 1985, vol. II, pp. 77–99.
5. Prasad, P., *Pitman Research Notes in Mathematics*, Longman, 1993, No. 293.
6. Prasad, P. and Sangeeta, K., *J. Fluid Mech.*, 1999, **385**, 1–20.
7. Monica, A. and Prasad, P., *Propagation of a curved weak shock front*, Preprint No. 01/1999, Department of Mathematics, Indian Institute of Science, Bangalore, communicated to *J. Fluid Mech.*
8. Prasad, P., *J. Indian Inst. Sci.*, 1995, **75**, 517–535.
9. Prasad, P., *J. Math. Anal. Appl.*, 1975, **50**, 470–482.
10. Prasad, P., *Wave Motion*, 1994, **20**, 21–31.
11. Morton, K. W., Prasad, P. and Ravindran, R., Technical Report 2, Department of Mathematics, Indian Institute of Science, Bangalore, 1992.
12. Courant, R. and Friedrichs, K. O., *Supersonic Flow and Shock Waves*, Interscience Publishers, reprinted by Springer Verlag, 1948.
13. Smoller, J., *Shock Waves and Reaction–Diffusion Equations*, Springer-Verlag, 1983.

ACKNOWLEDGEMENTS. This article is based on an unpublished work done by three students, namely S. Baskar and N. Potadar of the Department of Mathematics, IISc, Bangalore and Jérémie Szeftel of Ecole Normale Superieure, Lyon. I thank Prof. Renuka Ravindran, who jointly supervised the work of Jérémie and Potadar.

Received 3 May 2000; revised accepted 7 August 2000